

## Investigation of exciton fine structure in $\text{Cu}_2\text{O}$

Ch. Uihlein,\* D. Fröhlich, and R. Kenkies

*Institut für Physik, Universität Dortmund, 4600 Dortmund 50, Federal Republic of Germany*

(Received 25 August 1980)

The even-parity excitons in  $\text{Cu}_2\text{O}$  show, in contrast to the well known  $P$ -exciton series: (1) strong deviations from a hydrogenlike behavior, (2) a fine structure for  $n \geq 3$ , and (3) an unusual  $n$  dependence of the exchange splitting. All the properties of the even-parity-exciton series are explained by the presence of a strong  $H_d$  term and a strong exchange interaction. We have calculated the even- and odd-exciton members of the yellow and green series within the formalism of Baldereschi and Lipari. An excellent agreement with the experimental results is obtained in the spherical limit. The theory predicts for  $n = 3$  a splitting of the  $S$  and  $D$  states into five components. All the five components are observed by two-photon absorption in a magnetic field of 7 T.

### INTRODUCTION

After the first measurements by Hayashi and Katsuki<sup>1</sup> the excitons in  $\text{Cu}_2\text{O}$  were studied extensively by different groups for 30 years. Main contributions in this field in the following years were done by Gross and his co-workers in Leningrad<sup>2</sup> and Nikitine and his group in Strasbourg.<sup>3</sup> For literature we refer to a recent review article by Agekyan<sup>4</sup> and the paper by Washington *et al.*<sup>5</sup> on resonant Raman scattering in  $\text{Cu}_2\text{O}$ . From symmetry considerations Elliott<sup>6</sup> concluded that the upper valence band is of  $\Gamma_7^+$  and the lower of  $\Gamma_8^+$  symmetry. In a later band calculation of Dahl and Switendick,<sup>7</sup> the order of the spin-orbit components  $\Gamma_7^+$  and  $\Gamma_8^+$  of the  $\Gamma_5^+$  state ( $\text{Cu } 3d$ ) was reversed. A very recent band calculation by Kleinman and Mednick<sup>8</sup> confirms  $\Gamma_7^+$  as the uppermost valence band. With a  $\Gamma_6^+$  conduction band, both assignments correspond in one-photon absorption to the yellow and green  $P$ -exciton series which are very well resolved up to  $n = 10$ . Because of the perfect  $1/n^2$  dependence, the assignment of quantum numbers for the  $P$  states is unambiguous. As discussed in detail by Washington *et al.*<sup>5</sup> and lately by Fröhlich *et al.*,<sup>9</sup> the interpretation of the parity-forbidden  $S$  and  $D$  excitons is much more controversial. The spectrum of the even-parity excitons deviates drastically from a hydrogenic series. This fact led to contradicting assignments of quantum numbers. In addition there is a pronounced fine structure observed for  $n \geq 3$ , which has to be explained. Another problem is the large difference between the rydberg of the yellow and green series. In a naive analysis this would yield a factor of 1.5 between the reduced masses of the green and yellow series which can not be understood considering the rather small spin-orbit interaction. We will show that all these open questions can be answered by taking nondiagonal terms of the hole kinetic energy and exchange interaction

into account. As shown by Luttinger and Kohn<sup>10</sup> and by Baldereschi and Lipari,<sup>11</sup> the inclusion of nondiagonal terms in the effective-mass Hamiltonian is of considerable importance for the  $J = \frac{3}{2}$  ( $\Gamma_8$  in cubic symmetry) component of the spin-orbit doublet. This was recently demonstrated for the  $P$  excitons in  $\text{ZnSe}$  by Sondergeld and Stafford<sup>12</sup> and for  $\text{CuBr}$  by Mattausch and Uihlein.<sup>13</sup> In  $\text{Cu}_2\text{O}$  we have to consider the coupling between the  $J = \frac{1}{2}$  ( $\Gamma_7^+$  yellow series) and  $J = \frac{3}{2}$  ( $\Gamma_8^+$  green series) in order to explain the fine structure. This coupling is appreciable in the special case of  $\text{Cu}_2\text{O}$  because the  $1S$  green exciton happens to be almost degenerate with the higher excitons of the yellow series ( $n = 2, 3$ ). Our model Hamiltonian, which includes the spherical  $H_d$  term and exchange interaction, describes quantitatively all experimental findings. Additional lines in a magnetic field of 7 T are also explained.

### EXPERIMENT

The first two-photon absorption measurements on  $\text{Cu}_2\text{O}$  were done by Pradère *et al.*<sup>14</sup> Using a laser-induced flash or a flashlamp as a tunable source these authors were not able to resolve the fine structure. As discussed in detail by Fröhlich and Sondergeld,<sup>15</sup> the combination of a tunable low-power laser and a fixed-frequency high-power laser should yield a good signal-to-noise ratio and high resolution. The schematic diagram of our present setup is presented in Fig. 1. This setup differs from the standard setup as described before<sup>15</sup> in the following points:

(a) To account for higher repetition rates (5–10 pulses per second) we have included a specially designed microprocessor for a preaveraging of data, then to be handled by the desk-top calculator.

(b) Instead of a flashlamp and monochromator as a tunable source we use a tunable dye laser



any system with similar band structure. Adopting the formalism of Luttinger<sup>10</sup> and of Baldereschi and Lipari,<sup>11</sup> we treat in the following the threefold-degenerate valence band as having an effective spin 1. This allows us to introduce the quasi-spin operator  $\vec{I}$ , the magnetic quantum numbers of  $\vec{I}$  ( $m_I = \pm 1, 0$ ) referring to the different degenerate valence-band states without electron spin. To take into account the electron spin we introduce in addition the operators  $\vec{\sigma}_e$  and  $\vec{\sigma}_h$  for the electron and hole spin, respectively.

The Hamiltonian, which gives the exciton eigenstates, has to contain full information of the complex valence-band structure in the vicinity of the  $\Gamma$  point, the Coulomb interaction between electron and hole, and the electron-hole exchange interaction, which is large in the case of  $\text{Cu}_2\text{O}$ . Thus the Hamiltonian consists of the following terms:

$$\begin{aligned} H &= H_s + H_{so} + H_d + H_{\text{exch}}, \\ H_s &= \frac{1}{\hbar^2} p^2 - \frac{2}{r} - \bar{V}_0 \delta(\vec{r}), \\ H_{so} &= \frac{2}{3} \bar{\Delta} (1 + \vec{I} \cdot \vec{\sigma}_h), \\ H_d &= -\frac{\mu}{3\hbar^2} (P^{(2)} \cdot I^{(2)}), \\ H_{\text{exch}} &= \bar{J}_0 \left( \frac{1}{4} - \vec{\sigma}_e \cdot \vec{\sigma}_h \right) \delta(\vec{r}). \end{aligned} \quad (1)$$

The terms are given in reduced units  $R_0$  and  $a_0$  with zero energy at the band gap ( $\Gamma_7^+$  to  $\Gamma_8^+$ ). The parameters are defined as follows:

$$\begin{aligned} R_0 &= \frac{e^4 m_0}{2\hbar^2 \epsilon_0^2 \gamma_1'}, \quad a_0 = \frac{\hbar^2 \epsilon_0 \gamma_1'}{e^2 m_0}, \\ \mu &= \frac{6\gamma_3 + 4\gamma_2}{5\gamma_1'}, \quad \gamma_1' = \gamma_1 + \frac{m_0}{m_e}, \\ \bar{V}_0 &= \frac{V_0 \Omega}{R_0 a_0^3}, \quad \bar{\Delta} = \frac{\Delta}{R_0}, \quad \bar{J}_0 = \frac{J_0 \Omega}{R_0 a_0^3}. \end{aligned}$$

$\Omega$  is the volume of the unit cell, and  $J_0$  is the exchange integral and  $V_0$  the central-cell potential. The parameters  $\gamma_1$ ,  $\gamma_2$ , and  $\gamma_3$  are the dimensionless Luttinger parameters associated with the  $\Gamma_8^+$  valence band. In the limit of weak spin-orbit interaction, the parameter  $\gamma_1$  determines the inverse effective mass of the  $\Gamma_7^+$  band also.

$H_s$  is the usual hydrogenlike effective mass Hamiltonian for excitons in spite of a central-cell correction term. This term is introduced to account for all short-range deviations from a simple Coulomb potential, exciton-phonon interaction included. There exist other more sophisticated methods of treating the exciton-phonon interaction,<sup>17</sup> but they cannot be applied to the case of  $\text{Cu}_2\text{O}$  where one has two optical-phonon branches. We have therefore chosen the simplest type of short-range correction with the intention to fit

$V_0$  to the experimentally determined 1S exciton binding energy.

$H_{so}$  is an effective spin-orbit interaction term, giving rise to a splitting of the  $3 \times 2$ -fold-degenerate valence band ( $\Gamma_5^+$  in  $\text{Cu}_2\text{O}$ ) into a twofold-degenerate  $\Gamma_7^+$  and a fourfold-degenerate  $\Gamma_8^+$  component. The different valence-band components can be assigned by the quantum numbers of the effective hole spin  $\vec{J} = \vec{I} + \vec{\sigma}_h$ , which commutes with  $H_{so}$ . The two possible quantum numbers of  $J$ ,  $J = \frac{1}{2}$  and  $J = \frac{3}{2}$ , refer to the  $\Gamma_7^+$  and  $\Gamma_8^+$  valence band, respectively.

The sum of  $H_s$  and  $H_{so}$  describes two distinct, non-interacting, exciton series originating from the conduction band and the two spin-orbit split valence-band states (yellow and green series in  $\text{Cu}_2\text{O}$ ). The different exciton states can be classified by the quantum number  $J$  of the effective hole spin and the angular momentum  $L$  associated with the envelope function. We adopt in the following the atomic notation  $^{2J+1}L$ , where  $L$  refers to the symmetry of the envelope function ( $S, P, D, \dots$ ) and the superscript to the multiplicity of the valence band, thus distinguishing the two excitonic series.

The  $H_d$  term given in the notation of Baldereschi and Lipari<sup>11</sup> contains the nondiagonal  $d$ -like parts of the effective mass Hamiltonian in spherical approximation. The magnitude of this term is given by the dimensionless parameter  $\mu$  which weighs the ratio between the  $d$ -like and  $s$ -like parts of the kinetic energy. Neither  $\vec{J}$  nor  $\vec{L}$  commute with  $H_d$  and as a consequence the effective hole spin  $\vec{J}$  is now coupled to the angular momentum of the relative motion, thus giving rise to a fine-structure splitting for angular momentum states with  $L > 0$ . In the case of weak spin-orbit interaction the two excitonic series are in addition strongly mixed by the  $H_d$  term.  $L$  and  $J$  are therefore no longer good quantum numbers. The excitonic states have to be assigned instead by the quantum numbers of the angular momentum operator  $\vec{F} = \vec{L} + \vec{J}$ , which commutes with  $H_d$  in spherical approximation. Nevertheless it is useful to keep track of the approximate quantum numbers  $L$  and  $J$  which can be used to classify the states in addition, by regarding the limit  $\mu \rightarrow 0$ . Following the conventions for atomic states we therefore denote the excitons by  $^{2J+1}L_F$ , the subscript referring to the total angular momentum of the exciton without conduction-band spin. The Hamiltonian given by the sum of  $H_s + H_{so} + H_d$  is essentially the same as the one used by Baldereschi and Lipari.<sup>11</sup> In the case of  $\text{Cu}_2\text{O}$  one has to include in addition the exchange interaction between electron and hole. The exchange interaction, its magnitude being determined by the exchange integral  $J_0$ , gives rise to a

splitting of  $S$  excitons in ortho and para components. The radial dependence is approximated in  $H_{\text{exch}}$  by a  $\delta$  function, thus taking care of the fact that exchange depends on the probability of finding electron and hole within the same unit cell. The term is for this reason only nonzero for states having a component with angular momentum  $L=0$  ( $S$ -like envelope). The fact that neither  $J$  nor  $F$  commutes with  $H_{\text{exch}}$  has two consequences: (1) the two exciton series (yellow and green series in  $\text{Cu}_2\text{O}$ ) are mixed in addition by the exchange interaction, and (2)  $F$  is in general no longer a good quantum number. From the latter it follows that states have to be assigned now by the quantum numbers of  $\vec{F}_{\text{tot}} = \vec{F} + \vec{\sigma}_e$ , whenever a component with angular momentum  $L=0$  cannot be excluded by symmetry. The only states which can have an  $S$ -like admixture are states with angular momentum  $F = \frac{1}{2}$  ( $\Gamma_7^+$ ) and  $F = \frac{3}{2}$  ( $\Gamma_8^+$ ). Inclusion of the exchange interaction in the case  $F = \frac{1}{2}$  gives rise to a splitting into the para component  $F_{\text{tot}} = 0$  ( $\Gamma_2^+$ ) and the ortho component  $F_{\text{tot}} = 1$  ( $\Gamma_5^+$ ). For  $F = \frac{3}{2}$  one obtains the ortho- and para-exciton states  $F_{\text{tot}} = 1$  ( $\Gamma_5^+$ ) and  $F_{\text{tot}} = 2$  ( $\Gamma_3^+$ ,  $\Gamma_4^+$ ). In all other cases (odd-parity states and even-parity states with  $F > \frac{5}{2}$ ),  $F$  and  $M_F$  remain good quantum numbers. We can therefore distinguish two classes of excitons; i.e., ortho and para excitons which are denoted by an integer spin ( $F_{\text{tot}}$ ) and a second class of excitons which can be still classified by the half-integer spin  $F$ , because the electron spin is not coupled to the total angular momentum of envelope and hole.

The most general wave function which can be classified by the integer spin  $F_{\text{tot}}$  is a linear combination of the type

$$\psi = \sum_{L,J,F} g_{LJF}(r) |LJFF_{\text{tot}}M\rangle, \quad (2)$$

where  $g_{LJF}(r)$  are radial wave functions and  $|LJFF_{\text{tot}}M\rangle$  are angular and spin-dependent parts in the  $(I, \sigma_h; J)$ ,  $(L, J; F)(F, \sigma_e; F_{\text{tot}})$  coupling scheme. As is shown in the Appendix, an ansatz of this type leads to a set of coupled differential equations for the radial wave functions. These eigenvalue equations determine the binding energies of all excitons (ground and excited states) which are assigned by the same quantum number  $F_{\text{tot}}$ . Because of the selection rules for the spherical case, only a finite number of angular momentum parts contribute to a state with a given  $F_{\text{tot}}$ . The exciton binding energies are therefore completely determined by the finite sets of coupled differential equations listed in the Appendix. We solve these coupled eigenvalue equations by means of the finite-element method which is explained in detail in Ref. 13.

The treatment of the half-integer spin states ( $F$ ) is even more simple, since  $F$  is still a good quantum number. We use in this case an ansatz of the type

$$\psi = \sum_{L,J} g_{LJ}(r) |LJFM_F\rangle. \quad (3)$$

Because of selection rules the number of angular momentum states  $2J+1L_F$  contributing to a state with a given  $F$  is restricted in this case to a maximum of three. The coupled wave equations are again listed in the Appendix.

Odd-parity states containing a  $P$ -envelope contribution are expected to be electric dipole allowed. From group theory it follows that only the odd-parity states  $F = \frac{3}{2}$  and  $F = \frac{5}{2}$  contain the polar vector representation  $\Gamma_4^-$  when the conduction band of  $\Gamma_6^+$  symmetry is taken into account. One expects therefore one yellow series ( ${}^2P_{3/2}$ ) and two green series ( ${}^4P_{3/2}$  and  ${}^4P_{5/2}$ ) to be electric dipole allowed. Experimentally only one green series is observed. This discrepancy might indicate that interference effects with the continuum states of the yellow series give rise to a transfer of oscillator strength. As will be discussed in the next section (Table II), the experimental values are well explained by our calculation if we assume that the  ${}^2P_{3/2}$  and  ${}^4P_{3/2}$  excitons present the yellow and green series observed by one-photon absorption.

The spherical approximation accounts very well for the situation in  $\text{Cu}_2\text{O}$ . We will therefore discuss the influence of the cubic term only qualitatively. Coupling of the envelope angular momentum and the effective hole spin ( $\Gamma_7^+$ ,  $\Gamma_8^+$ ) yields even- and odd-parity states transforming according to  $\Gamma_6$ ,  $\Gamma_7$ , and  $\Gamma_8$ . Exchange interaction affects only the even-parity states  $\Gamma_7^+$  and  $\Gamma_8^+$ . Coupling with the electron spin ( $\Gamma_6^+$ ) yields in turn the ortho excitons  $\Gamma_5^+$  and the para excitons  $\Gamma_2^+$  and ( $\Gamma_3^+$ ,  $\Gamma_4^+$ ), the latter ones being degenerate in the spherical approximation of the exchange interaction. In the extreme cubic limit one can therefore only distinguish between odd-parity states  $\Gamma_6^-$ ,  $\Gamma_7^-$ , and  $\Gamma_8^-$ , even-parity states  $\Gamma_6^+$ , ortho excitons  $\Gamma_5^+$ , and para excitons  $\Gamma_2^+$  and ( $\Gamma_3^+$ ,  $\Gamma_4^+$ ). In the case of a small cubic contribution, however, one can treat the cubic term as a weak perturbation of the spherical case. The cubic term affects then the exciton members stemming from the  $\Gamma_8^+$  valence band ( $J = \frac{3}{2}$ ) and the  $\Gamma_7^+$  valence band ( $J = \frac{1}{2}$ ) in a different way. The contribution of the cubic  $H_4$  term relative to the spherical one depends in the first case on the ratio  $\delta : \mu$ , in the latter one on  $\delta^2 : \mu^2$ . This follows from the fact that the  $H_4$  terms contribute to the  $J = \frac{3}{2}$  exciton series in first order (intra-band terms) and to the  $J = \frac{1}{2}$  exciton

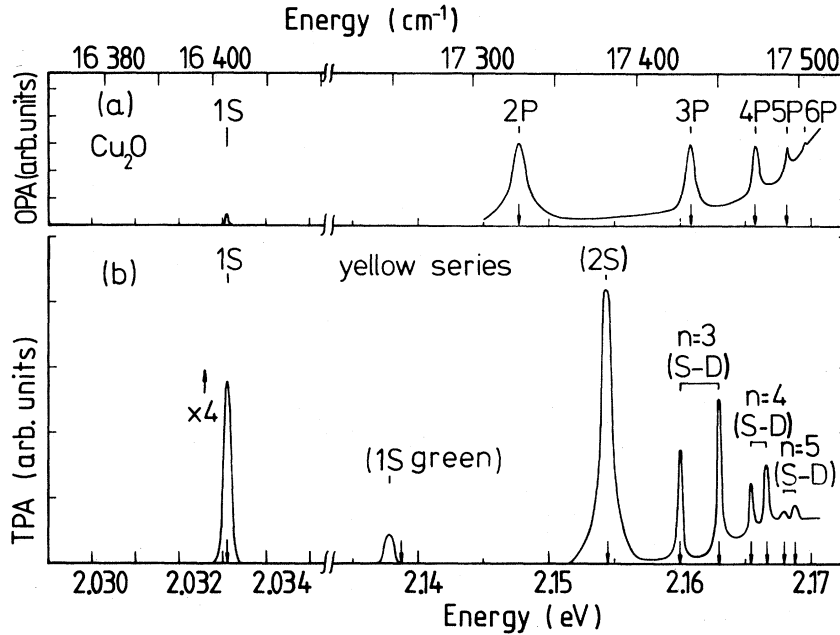


FIG. 2. One- and two-photon spectra of  $\text{Cu}_2\text{O}$ . (a) One-photon data at 4.2 K from Ref. 20; (b) two-photon data at 4.5 K. The yellow 1S exciton line was measured at 20 K. The arrows indicate the calculated exciton energies.

series in second order (interband terms). The  $J = \frac{1}{2}$  exciton series (yellow series in  $\text{Cu}_2\text{O}$ ) is therefore much better described within a spherical model than the  $J = \frac{3}{2}$  exciton series (green series in  $\text{Cu}_2\text{O}$ ).

#### EXPERIMENTAL RESULTS AND DISCUSSION

In this section we will present the experimental findings for  $\text{Cu}_2\text{O}$  as obtained by one-photon (OPA) and two-photon (TPA) absorption. The experimental results are compared to energy values calculated within the preceding model with a best set of parameters. Figure 2 shows the spectrum of the even-parity excitons up to  $n = 5$  as measured by TPA. For comparison the odd-parity excitons up to  $n = 6$  as measured by the Strasbourg group<sup>18</sup> by OPA (one-photon absorption) are also reproduced. As discussed by us in detail in the preceding letter,<sup>9</sup> the controversy concerning the assignment of the main quantum numbers  $n$  for the even-parity excitons is now settled. One of the main reasons why this controversy lasted so long is the fact that the "2S" line is found on the high-energy side of the 2P line, whereas one would expect it to be shifted to lower energies.

We have calculated all the even- and odd-parity states of the yellow and green series up to  $F_{\text{tot}} = 2$ ,  $F = \frac{5}{2}$ , and  $n = 5$  using the following set of parameters:

$$R_0 = 0.087 \text{ eV}; \quad \mu = 0.47; \quad E_{\text{gap}} = 2.1720 \text{ eV}; \\ \Delta = 0.1338 \text{ eV}; \quad \bar{V}_0 = 0.53; \quad \bar{J}_0 = 0.58.$$

The results of our calculation are listed in Tables I and II. As one can see, the agreement between experiment and theory is excellent. In the case of the even-parity states we have listed in addition the composition of the wave functions. The assignment of the different states refers always to the limit  $\mu \rightarrow 0$  and  $J_0 \rightarrow 0$ . This has to be considered when one compares the composition of the 1S-green and 2S-yellow excitons.

It was demonstrated in the preceding letter<sup>9</sup> that only the ortho excitons ( $F_{\text{tot}} = 1$ ) are observed in a two-photon absorption experiment ( $\Gamma_5^+$  states are direct two-photon allowed). The spherical model explains the occurrence of ortho-exciton doublets for  $n \geq 3$ . Our theory predicts for  $n = 3$  (yellow series) a total of five different exciton states, the remaining ones being the para-exciton states  $F_{\text{tot}} = 0$  ( $\Gamma_2^+$ ) and  $F_{\text{tot}} = 2$  ( $\Gamma_3^+$ ,  $\Gamma_4^+$ ), and the half-integer spin state  ${}^2D_{5/2}$ . TPA measurements in a magnetic field (up to 8.5 T) yield these additional lines as is shown in Fig. 3. The magnetic field measurements were done in Faraday configuration with magnetic field parallel to a [100] direction. Contrary to one-photon experiments, TPA in Faraday configuration will yield for this orientation only states with  $M = 0$ . The three additional lines become allowed by magnetic field interaction

TABLE I. Excitation energies and decomposition into relevant basis states of even-parity excitons in  $\text{Cu}_2\text{O}$ .

State <sup>a</sup>	$E_{\text{expt}}$ (eV) <sup>b</sup>	$E_{\text{calc}}$ (eV) <sup>c</sup>	${}^2S_{1/2}$	${}^4D_{1/2}$	${}^4S_{3/2}$	${}^2D_{3/2}$	${}^4D_{3/2}$
$F_{\text{tot}}=1$ ortho excitons							
1 ${}^2S_{1/2}$	2.0330	2.0330	0.91	0.06	0.03	0.00	0.00
1 ${}^4S_{3/2}$	2.1378	2.1388	0.88	0.02	0.08	0.02	0.00
2 ${}^2S_{1/2}$	2.1544	2.1552	0.35	0.00	0.32	0.32	0.01
3 ${}^2S_{1/2}$	2.1603	2.1600	0.72	0.01	0.03	0.24	0.00
3 ${}^2D_{3/2}$	2.1630	2.1632	0.18	0.00	0.06	0.76	0.00
4 ${}^2S_{1/2}$	2.1653	2.1654	0.83	0.00	0.01	0.16	0.00
4 ${}^2D_{3/2}$	2.1666	2.1668	0.15	0.00	0.02	0.83	0.00
5 ${}^2S_{1/2}$	2.1678	2.1679	0.85	0.00	0.01	0.14	0.00
5 ${}^2D_{3/2}$	2.1685	2.1686	0.14	0.00	0.01	0.85	0.00
$F_{\text{tot}}=0$ para excitons							
1 ${}^2S_{1/2}$	2.0212 <sup>d</sup>	2.0212	0.93	0.07			
2 ${}^2S_{1/2}$		2.1395	0.98	0.02			
3 ${}^2S_{1/2}$	2.1589 <sup>f</sup>	2.1589	0.99	0.01			
4 ${}^2S_{1/2}$		2.1651	1.00	0.00			
5 ${}^2S_{1/2}$		2.1677	1.00	0.00			
$F_{\text{tot}}=2$ para excitons							
1 ${}^4S_{3/2}$	2.1269 <sup>e</sup>	2.1305			0.78	0.20	0.02
3 ${}^2D_{3/2}$	2.1624 <sup>f</sup>	2.1621			0.01	0.99	0.00
4 ${}^2D_{3/2}$		2.1664			0.00	1.00	0.00
5 ${}^2D_{3/2}$		2.1684			0.00	1.00	0.00
$F=\frac{5}{2}$ excitons							
3 ${}^2D_{5/2}$	2.1619 <sup>f</sup>	2.1618	${}^2D_{5/2}$	${}^4D_{5/2}$	${}^4G_{5/2}$		
4 ${}^2D_{5/2}$		2.1662	1.00	0.00	0.00		
5 ${}^2D_{5/2}$		2.1683	1.00	0.00	0.00		

<sup>a</sup> Symmetry assignment referring to the limit  $\mu \rightarrow 0$  and  $J_0 \rightarrow 0$ .

<sup>b</sup> Energies as obtained by TPA.

<sup>c</sup> Energies calculated within our model.

<sup>d</sup> Triplet exciton energy according to Ref. 21.

<sup>e</sup> Triplet exciton energy according to Ref. 22.

<sup>f</sup> Energies as obtained by TPA magneto-optic experiments.

TABLE II. Excitation energies of the odd-parity excitons  ${}^2P_{3/2}$  and  ${}^4P_{3/2}$  in  $\text{Cu}_2\text{O}$ .

State <sup>a</sup>	$E_{\text{expt}}$ (eV) <sup>b</sup>	$E_{\text{calc}}$ (eV) <sup>c</sup>
2 $P Y$	2.1473	2.1473
3 $P Y$	2.1609	2.1610
4 $P Y$	2.1657	2.1659
5 $P Y$	2.1680	2.1681
2 $P G$	2.2679	2.2677
3 $P G$	2.2889	2.2887
4 $P G$	2.2963	2.2960
5 $P G$	2.2997	2.2995

<sup>a</sup> Symmetry assignment;  $Y$  and  $G$  refer to the yellow and green series, respectively.

<sup>b</sup> Energies of  $\Gamma_4^-$  excitons as obtained by one-photon absorption according to Ref. 5 and literature cited therein.

<sup>c</sup> Energies calculated as shown in the text.

with the ortho-exciton components. As indicated in Fig. 3, most of the experimental lines are shifted to higher energies as compared to the theoretical results. This can be qualitatively explained by the diamagnetic shift of the  $M=0$  states which was not taken into account in our calculation. The splitting pattern for  $n=3$ , as induced by the different terms of the Hamiltonian, is schematically depicted in Fig. 4. A detailed analysis of the field dependence of the lines as well as additional measurements in Voigt configuration and possibly other crystalline orientations, should yield further information on the magnetic properties of the even-parity excitons.

Our model explains for the first time all the interesting features of the even-parity-exciton states in  $\text{Cu}_2\text{O}$ ; i.e., (1) the non-hydrogen-like behavior of the exciton series, (2) the fine-structure splitting for  $n \geq 3$ ; (3) the puzzling  $n$  depen-

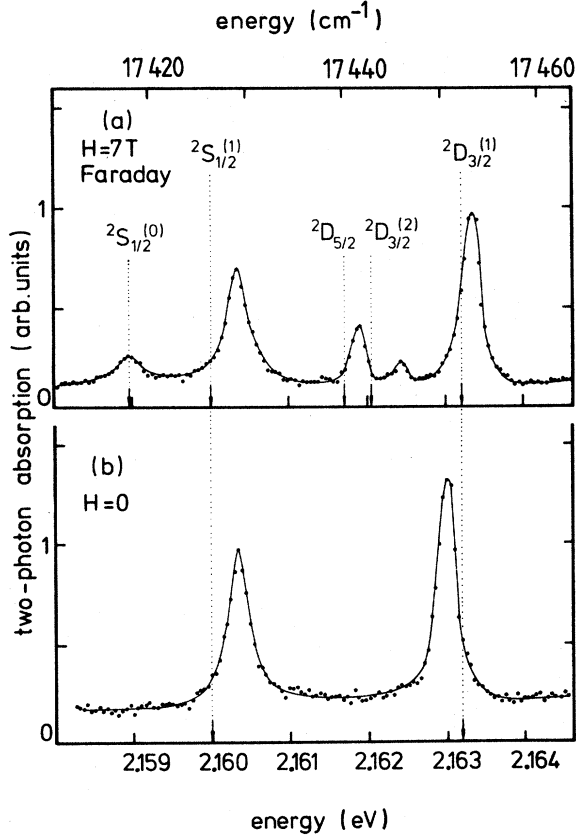


FIG. 3. Two-photon spectra of the  $n=3$  exciton fine structure at 4.5 K of  $\text{Cu}_2\text{O}$ . (a)  $H=7$  T; (b)  $H=0$  T. The spectra were obtained with both beams being circularly polarized with the same helicity. The dotted lines indicate the calculated exciton energies. The quantum numbers are used as in Table I with  $F_{\text{tot}}=0, 1$ , or  $2$  given in brackets.

dence of the exchange splitting which has prevented the assignment of exciton states for such a long time. Our results demonstrate in addition that the cubic contribution is weak. A large cubic  $H_d$  term would split the  ${}^2D_{5/2}$  exciton state into a  $\Gamma_6^+$  and  $\Gamma_8^+$  component, the  $\Gamma_8^+$  component strongly interacting with the  ${}^4S_{3/2}(\Gamma_8^+)$  state. Exchange interaction would in turn split the  ${}^2D_{5/2}(\Gamma_8^+)$  component by its  ${}^4S_{3/2}$  admixture into a para component

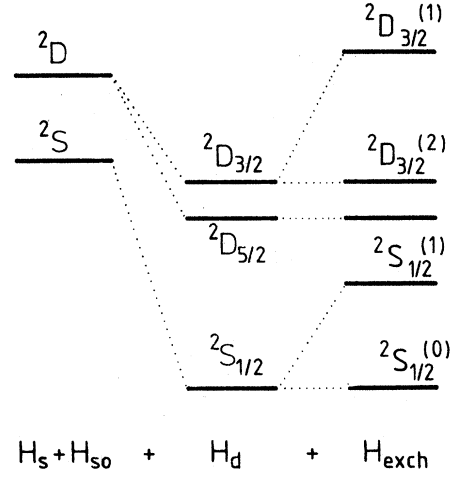


FIG. 4. Schematic representation of the fine-structure splitting of the  $n=3$  state (yellow series).

( $\Gamma_3^+, \Gamma_4^+$ ) and into an ortho component  $\Gamma_5^+$ . In the extreme cubic limit one would therefore expect to observe three two-photon-allowed  $\Gamma_5^+$  states for  $n=3$  instead of only two lines, and within a magnetic field seven lines instead of only five lines.

#### APPENDIX

We now list the differential equations for the radial wave functions. In deriving these equations we follow very closely the procedure of Baldereschi and Lipari (BL).<sup>11</sup> The binding energy of an exciton state is given with respect to the  $\Gamma_5^+ - \Gamma_6^+$  band gap by the equation  $H\psi = -E\psi$  where

$$\psi = \sum_{L', J', F'} g_{L'J'F'}(r) |L'J'F'F_{\text{tot}}M\rangle.$$

Multiplying from the left with  $|LJFF_{\text{tot}}M\rangle$  and integration over angular and spin-dependent parts yields

$$\sum_{L', J', F'} \langle LJFF_{\text{tot}}M | H | L'J'F'F_{\text{tot}}M \rangle g_{L'J'F'}(r) + E g_{LJF}(r) = 0. \quad (\text{A1})$$

The matrix elements of  $H$  can be calculated by the reduced-matrix-element technique.<sup>19</sup> One obtains for the different parts of the Hamiltonian the re-

$$\langle LJFF_{\text{tot}}M | \left[ \frac{1}{\hbar^2} p^2 - \frac{2}{r} \right] | L'J'F'F_{\text{tot}}M \rangle = \delta_{LL'} \delta_{JJ'} \delta_{FF'} \left( -\frac{d^2}{dr^2} - \frac{2}{r} \frac{d}{dr} + \frac{L(L+1)}{r^2} - \frac{2}{r} \right), \quad (\text{A2})$$

$$\langle LJFF_{\text{tot}}M | (P^{(2)} \cdot I^{(2)}) | L'J'F'F_{\text{tot}}M \rangle = \delta_{FF'} (-1)^{F+L'+J+J'+I+\sigma_h} [(2J+1)(2J'+1)]^{1/2} \\ \times \left\{ \begin{matrix} L & 2 & L' \\ J & F & J' \end{matrix} \right\} \left\{ \begin{matrix} I & 2 & I \\ J & \sigma_h & J' \end{matrix} \right\} (I \| I^{(2)} \| I) (L \| P^{(2)} \| L'), \quad (\text{A3})$$

$$\langle L J F F_{\text{tot}} M | \vec{1} \cdot \vec{\sigma}_h | L' J' F' F_{\text{tot}} M \rangle = \delta_{LL'} \delta_{JJ'} \delta_{FF'} \frac{1}{2} [J(J+1) - I(I+1) - \sigma_h(\sigma_h+1)] \quad (\text{A4})$$

$$\begin{aligned} & \langle L J F F_{\text{tot}} M | \vec{\sigma}_e \cdot \vec{\sigma}_h \delta(\vec{r}) | L' J' F' F_{\text{tot}} M \rangle \\ &= \delta_{LL'} (-1)^{F_{\text{tot}} + 2F' + 2J + L + I + \sigma_e + \sigma_h} [(2F+1)(2F'+1)]^{1/2} \\ & \times [(2J+1)(2J'+1)]^{1/2} \begin{Bmatrix} F & 1 & F' \\ \frac{1}{2} & F_{\text{tot}} & \frac{1}{2} \end{Bmatrix} \begin{Bmatrix} J & 1 & J' \\ F' & L & F \end{Bmatrix} \begin{Bmatrix} \frac{1}{2} & 1 & \frac{1}{2} \\ J' & 1 & J \end{Bmatrix} (\vec{\sigma}_e \parallel \vec{\sigma}_e \parallel \vec{\sigma}_e) (\vec{\sigma}_h \parallel \vec{\sigma}_h \parallel \vec{\sigma}_h) (L \parallel \delta \parallel L). \end{aligned} \quad (\text{A5})$$

The reduced matrix element of the  $\delta$  function is zero for  $L \neq 0$ . For  $L = 0$  we use in the following the abbreviation  $\hat{\delta}(r)$ . This reduced matrix element is defined by the relation

$$4\pi \int r^2 \hat{\delta}(r) f(r) dr = f(0). \quad (\text{A6})$$

A representation of  $\hat{\delta}(r)$  is the step function which is  $1/\Omega$  within a sphere of volume  $\Omega$  and zero elsewhere. The distribution  $\hat{\delta}(r)$  is approached in the limit  $\Omega \rightarrow 0$ , but for actual calculations one can choose  $\Omega$  to be the volume of the unit cell. The  $6j$  symbols occurring in Eqs. (A3) and (A5) are tabulated by Rotenberg<sup>20</sup> and the reduced matrix elements ( $I \parallel I^{(2)} \parallel I$ ) and ( $L \parallel P^{(2)} \parallel L'$ ) are listed in the paper of BL.<sup>11</sup> The reduced matrix element of the spin operator is

$$(\sigma \parallel \sigma \parallel \sigma) = [\sigma(\sigma+1)(2\sigma+1)]^{1/2} = \sqrt{3/2}.$$

Considering the matrix elements (A2) to (A5) we deduce immediately the following properties:

- (1)  $H_s$  contributes only diagonal terms.
- (2)  $H_d$  (spherical approximation) is diagonal with respect to  $F$ . Because of parity and the triangle condition of angular momentum coupling, we have in addition  $\Delta L = 0, \pm 2$ .
- (3)  $H_{s0}$  contributes only diagonal terms.
- (4)  $H_{\text{exch}}$  is diagonal with respect to  $L$ . Because of the  $\delta$  function only  $S$  states have to be considered.

We now list the most general wave functions and the differential equations for the odd-parity states  $F = \frac{1}{2}$ ,  $F = \frac{3}{2}$ , and  $F = \frac{5}{2}$ . For convenience, we introduce  $P_{LL'}$  as an abbreviation for differential operators associated with the reduced matrix elements of the kinetic energy terms.  $P_{LL'}$  is defined by the equations

$$\begin{aligned} P_{L-2,L} &= \frac{d^2}{dr^2} + \frac{2L+1}{r} \frac{d}{dr} + \frac{L^2-1}{r^2}, \\ P_{L,L} &= \frac{d^2}{dr^2} + \frac{2}{r} \frac{d}{dr} - \frac{L(L+1)}{r^2}, \\ P_{L+2,L} &= \frac{d^2}{dr^2} - \frac{2L+1}{r} \frac{d}{dr} + \frac{L(L+2)}{r^2}, \end{aligned} \quad (\text{A7})$$

$F = \frac{1}{2}$ :

$$\begin{aligned} \psi &= g_1(r)^2 P_{1/2} + g_2(r)^4 P_{1/2}, \\ \begin{vmatrix} P_{11} + \frac{2}{r} - E & -\sqrt{2}\mu P_{11} \\ -\sqrt{2}\mu P_{11} & (1+\mu)P_{11} + \frac{2}{r} - \bar{\Delta} - E \end{vmatrix} \begin{vmatrix} g_1(r) \\ g_2(r) \end{vmatrix} &= 0, \end{aligned} \quad (\text{A8})$$

$F = \frac{3}{2}$ :

$$\begin{aligned} \psi &= g_1(r)^2 P_{3/2} + g_2(r)^4 P_{3/2} + g_3(r)^4 F_{3/2}, \\ \begin{vmatrix} P_{11} + \frac{2}{r} - E & \frac{1}{\sqrt{5}}\mu P_{11} & -\frac{3}{\sqrt{5}}\mu P_{13} \\ \frac{1}{\sqrt{5}}\mu P_{11} & (1 - \frac{4}{5}\mu)P_{11} + \frac{2}{r} - \bar{\Delta} - E & -\frac{3}{5}\mu P_{13} \\ -\frac{3}{\sqrt{5}}\mu P_{31} & -\frac{3}{5}\mu P_{31} & (1 + \frac{4}{5}\mu)P_{33} + \frac{2}{r} - \bar{\Delta} - E \end{vmatrix} \begin{vmatrix} g_1(r) \\ g_2(r) \\ g_3(r) \end{vmatrix} &= 0, \end{aligned} \quad (\text{A9})$$

$F = \frac{5}{2}$ :

$$\psi = g_1(r)^4 P_{5/2} + g_2(r)^2 F_{5/2} + g_3(r)^4 F_{5/2}, \quad (\text{A10})$$

$$\begin{vmatrix} (1 + \frac{1}{5}\mu)P_{11} + \frac{2}{\gamma} - \bar{\Delta} - E & \sqrt{\frac{6}{5}}\mu P_{13} & -\frac{2}{5}\sqrt{6}\mu P_{13} \\ \sqrt{\frac{6}{5}}\mu P_{31} & P_{33} + \frac{2}{\gamma} - E & -\frac{2}{\sqrt{5}}\mu P_{33} \\ -\frac{2}{5}\sqrt{6}\mu P_{31} & -\frac{2}{\sqrt{5}}\mu P_{33} & (1 - \frac{1}{5}\mu)P_{33} + \frac{2}{\gamma} - \bar{\Delta} - E \end{vmatrix} \begin{vmatrix} g_1(r) \\ g_2(r) \\ g_3(r) \end{vmatrix} = 0.$$

We next list the differential equations for the even-parity excitons. We start with the para-exciton states  $F_{\text{tot}} = 0 (\Gamma_2^+)$  and  $F_{\text{tot}} = 2 (\Gamma_3^+, \Gamma_4^+)$ :

$F_{\text{tot}} = 0$ :

$$\psi = g_1(r)^2 S_{1/2} + g_2(r)^4 D_{1/2}, \quad (\text{A11})$$

$$\begin{vmatrix} P_{00} + \frac{2}{\gamma} + \bar{V}_0 \hat{\delta}(r) - E & -\sqrt{2}\mu P_{02} \\ -\sqrt{2}\mu P_{20} & (1 + \mu)P_{22} + \frac{2}{\gamma} - \bar{\Delta} - E \end{vmatrix} \begin{vmatrix} g_1(r) \\ g_2(r) \end{vmatrix} = 0,$$

$F_{\text{tot}} = 2 (F = \frac{3}{2})$ :

$$\psi = g_1(r)^4 S_{3/2} + g_2(r)^2 D_{3/2} + g_3(r)^4 D_{3/2}, \quad (\text{A12})$$

$$\begin{vmatrix} P_{00} + \frac{2}{\gamma} + \bar{V}_0 \hat{\delta}(r) - \bar{\Delta} - E & \mu P_{02} & -\mu P_{02} \\ \mu P_{20} & P_{22} + \frac{2}{\gamma} - E & -\mu P_{22} \\ -\mu P_{20} & -\mu P_{22} & P_{22} + \frac{2}{\gamma} - \bar{\Delta} - E \end{vmatrix} \begin{vmatrix} g_1(r) \\ g_2(r) \\ g_3(r) \end{vmatrix} = 0.$$

The differential equations for the ortho excitons are the same as for the para excitons besides the additional exchange term. The  $F_{\text{tot}} = 1$  matrix (5×5) can thus be deduced from the  $F_{\text{tot}} = 0$  and  $F_{\text{tot}} = 2$  matrices by adding the exchange matrix

$F_{\text{tot}} = 1$ :

$$\psi = g_1(r)^2 S_{1/2} + g_2(r)^4 D_{1/2} + g_3(r)^4 S_{3/2} + g_4(r)^2 D_{3/2} + g_5(r)^4 D_{3/2}, \quad (\text{A13})$$

$$\begin{vmatrix} F_{\text{tot}}=0 & 0 \\ & F_{\text{tot}}=2 \end{vmatrix} + \begin{vmatrix} -\frac{1}{3}\bar{J}_0 \hat{\delta}(r) & 0 & \frac{\sqrt{2}}{3}\bar{J}_0 \hat{\delta}(r) & 0 & 0 \\ 0 & 0 & 0 & 0 & 0 \\ \frac{\sqrt{2}}{3}\bar{J}_0 \hat{\delta}(r) & 0 & -\frac{2}{3}\bar{J}_0 \hat{\delta}(r) & 0 & 0 \\ 0 & 0 & 0 & 0 & 0 \\ 0 & 0 & 0 & 0 & 0 \end{vmatrix}.$$

From the even-parity states which can be denoted by half-integer spin, we are only interested in the  $F = \frac{5}{2}$  states:

$F = \frac{5}{2}$ :

$$\psi = g_1(r)^2 D_{5/2} + g_2(r)^4 D_{5/2} + g_3(r)^4 G_{5/2}, \quad (\text{A14})$$

$$\begin{vmatrix} P_{22} + \frac{2}{\gamma} - E & \sqrt{\frac{2}{7}}\mu P_{22} & -2\sqrt{\frac{3}{7}}\mu P_{24} \\ \sqrt{\frac{2}{7}}\mu P_{22} & (1 - \frac{5}{7}\mu)P_{22} + \frac{2}{\gamma} - \bar{\Delta} - E & -\frac{2}{7}\sqrt{6}\mu P_{24} \\ -2\sqrt{\frac{3}{7}}\mu P_{42} & -\frac{2}{7}\sqrt{6}\mu P_{42} & (1 + \frac{5}{7}\mu)P_{44} + \frac{2}{\gamma} - \bar{\Delta} - E \end{vmatrix} \begin{vmatrix} g_1(r) \\ g_2(r) \\ g_3(r) \end{vmatrix} = 0.$$

- \*Present address: Hochfeldmagnetlabor MPIF, 166x, F-38042 Grenoble Cédex, France.
- <sup>1</sup>M. Hayashi and K. Katsuki, *J. Phys. Soc. Jpn.* **5**, 380 (1950); **7**, 599 (1952).
- <sup>2</sup>E. F. Gross, *Usp. Fiz. Nauk* **76**, 433 (1962) [Sov. Phys.—Usp. **5**, 195 (1962)], and references cited.
- <sup>3</sup>S. Nikitine, *Prog. Semicond.* **6**, 235 (1962); in *Optical Properties of Solids*, edited by S. Nudelman and S. S. Mitra (Plenum, New York, 1969), p. 197; J. C. Merle, C. Wecker, A. Daunois, J. L. Deiss, and S. Nikitine, *Surf. Sci.* **37**, 347 (1973).
- <sup>4</sup>V. T. Agekyan, *Phys. Status Solidi A* **43**, 11 (1977).
- <sup>5</sup>M. A. Washington, A. Z. Genack, H. Z. Cummins, R. H. Bruce, A. Compaan, and R. A. Forman, *Phys. Rev. B* **15**, 2145 (1977).
- <sup>6</sup>R. J. Elliott, *Phys. Rev.* **124**, 340 (1961).
- <sup>7</sup>J. P. Dahl and A. C. Switendick, *J. Phys. Chem. Solids*, **27**, 931 (1966).
- <sup>8</sup>L. Kleinman and K. Mednick, *Phys. Rev. B* **21**, 1549 (1979).
- <sup>9</sup>D. Fröhlich, R. Kenklies, Ch. Uihlein, and C. Schwab, *Phys. Rev. Lett.* **43**, 1260 (1979).
- <sup>10</sup>J. M. Luttinger and W. Kohn, *Phys. Rev.* **97**, 869 (1955).
- <sup>11</sup>A. Baldereschi and N. O. Lipari, *Phys. Rev. B* **8**, 2697 (1973); N. O. Lipari and A. Baldereschi, *Solid State Commun.* **25**, 665 (1978).
- <sup>12</sup>M. Sondergeld and R. G. Stafford, *Phys. Rev. Lett.* **35**, 1529 (1975); M. Sondergeld, *Phys. Status Solidi B* **81**, 253 (1977); **81**, 451 (1977).
- <sup>13</sup>H. J. Mattausch and Ch. Uihlein, *Phys. Status Solidi B* **96**, 189 (1979).
- <sup>14</sup>F. Pradère, B. Sacks, and A. Mysyrowicz, *Opt. Commun.* **1**, 234 (1969); F. Pradère, A. Mysyrowicz, K. C. Rustagi, and D. Trivich, *Phys. Rev. B* **4**, 3570 (1971); K. C. Rustagi, F. Pradère, and A. Mysyrowicz, *ibid.* **8**, 2721 (1973).
- <sup>15</sup>D. Fröhlich and M. Sondergeld, *J. Phys. E* **10**, 761 (1977).
- <sup>16</sup>The crystals were kindly supplied by Dr. C. Schwab, Université Louis Pasteur, Strasbourg, France.
- <sup>17</sup>H. -R. Trebin, *Phys. Status Solidi B* **92**, 601 (1979).
- <sup>18</sup>J. B. Grun and S. Nikitine, *J. Phys. (Paris)* **23**, 159 (1962); S. Nikitine, J. B. Grun, and M. Certier, *Phys. Kondens. Mater.* **1**, 214 (1963).
- <sup>19</sup>A. R. Edmonds, *Angular Momentum in Quantum Mechanics* (Princeton University Press, Princeton, New Jersey, 1960); A. Messiah, *Quantum Mechanics* (North-Holland, Amsterdam, 1961).
- <sup>20</sup>M. Rotenberg, R. Bivins, N. Metropolis, and J. K. Wooten, *The 3-j and 6-j Symbols* (MIT Press, Cambridge, Mass., 1959).
- <sup>21</sup>P. D. Bloch and C. Schwab, *Phys. Rev. Lett.* **41**, 514 (1978).
- <sup>22</sup>V. T. Agekyan and Yu. A. Stepanov, *Fiz. Tverd. Tela* **17**, 1592 (1975) [Sov. Phys.—Solid State **17**, 1041 (1975)].